Structure
Article

Crystal Structure of NFAT Bound to the HIV-1 LTR Tandem κB Enhancer Element

Darren L. Bates,[1] Kristen K.B. Barthel,[1] Yongqing Wu,[2] Reza Kalhor,[2] James C. Stroud,[1] Michael J. Giffin,[1] and Lin Chen[2,*]
[1]Department of Chemistry and Biochemistry, University of Colorado at Boulder, Boulder, CO 80309-0215, USA
[2]Molecular and Computational Biology, Department of Chemistry, Norris Cancer Center, University of Southern California, Los Angeles, CA 90089-2910, USA
*Correspondence: linchen@usc.edu
DOI 10.1016/j.str.2008.01.020

SUMMARY

The host factor, nuclear factor of activated T-cells (NFAT), regulates the transcription and replication of HIV-1. Here, we have determined the crystal structure of the DNA binding domain of NFAT bound to the HIV-1 long terminal repeat (LTR) tandem κB enhancer element at 3.05 Å resolution. NFAT binds as a dimer to the upstream κB site (Core II), but as a monomer to the 3′ end of the downstream κB site (Core I). The DNA shows a significant bend near the 5′ end of Core I, where a lysine residue from NFAT bound to the 3′ end of Core II inserts into the minor groove and seems to cause DNA bases to flip out. Consistent with this structural feature, the 5′ end of Core I become hypersensitive to dimethylsulfate in the in vivo footprinting upon transcriptional activation of the HIV-1 LTR. Our studies provide a basis for further investigating the functional mechanisms of NFAT in HIV-1 transcription and replication.

INTRODUCTION

HIV-1 pathogenesis correlates closely with replication efficiency in infected host cells (Michael et al., 1992; Piatak et al., 1993), which is regulated by a complex interaction between viral and cellular factors (Choi et al., 2005; Cicala et al., 2006; Fenard et al., 2005; Pereira et al., 2000; Pessler and Cron, 2004). HIV-1 preferentially replicates in proliferating $CD4^+$ T cells, partly by taking advantage of the activated host transcription machinery (Levine et al., 1996; Siekevitz et al., 1987; Weissman et al., 1996). HIV-1 also seems to be able to induce cellular signals in nonproliferating target cells that allow low-level viral replication in the absence of cellular proliferation (Bounou et al., 2001; Choi et al., 2005; Cicala et al., 2002, 2006; Greene, 1990; Robichaud et al., 2002; Simmons et al., 2001), a mechanism thought to play a role in the establishment and maintenance of viral latency. A major regulatory step of HIV-1 replication is transcriptional initiation from the long terminal repeat (LTR) of HIV-1. The LTR contains many *cis*-acting DNA sequences linked to the regulation of HIV-1 transcription (Jeeninga et al., 2000).

Among the *cis*-acting DNA sequences on the HIV-1 LTR, the regulatory region between nucleotides −104 and −80 is the most extensively characterized (Cron et al., 2000; Kawakami et al., 1988; Kinoshita et al., 1997; Nabel and Baltimore, 1987; Perkins et al., 1993). Substantial evidence suggests that this region and the adjacent three Sp-1 sites are important for HIV-1 transcription. The region spanning −104 to −80 contains two consensus nuclear factor (NF)-κB binding sites (HIV-1 κB site) that are identical to the κB site found on the promoter of the immunoglobulin (Ig) κ light chain gene, also known as the Ig κB site. The upstream and downstream κB sites on the HIV-1 LTR have identical core sequences, and are referred to as Core II and Core I, respectively. The sequences of the κB sites and the four nucleotide spacer are highly conserved on most isolates of HIV-1 (Jeeninga et al., 2000; Verhoef et al., 1999). Deletion and site-directed mutation of these κB sites abolish reporter gene activation driven by the HIV-1 LTR (Cron et al., 2000; Kawakami et al., 1988; Kinoshita et al., 1997; Nabel and Baltimore, 1987; Perkins et al., 1993). Despite earlier conflicting results (Leonard et al., 1989; Ross et al., 1991), later studies strongly suggest that HIV-1 uses the conserved κB sites to enhance its replication in infected host cells (Alcami et al., 1995; Chen et al., 1997).

In addition to NF-κB, increasing evidence suggests that the related rel family transcription factor nuclear factor of activated T-cells (NFAT) is also involved in HIV-1 transcription. NFAT was originally characterized as a transcription factor important for the expression of the interleukin (IL)-2 gene (McCaffrey et al., 1993; Northrop et al., 1994; Shaw et al., 1988). Its function has now been expanded to the regulation of diverse genes both within and beyond the immune system (Crabtree and Olson, 2002; Hogan et al., 2003). The prototypical NFAT family of transcription factors (NFAT1–4) contains an N-terminal calcineurin binding domain, a DNA binding domain (also known as the rel homology region [RHR]), and a C-terminal transactivation domain. NFAT family members often cooperate with other transcription factors, such as AP-1, GATA, MEF2, and FOXP, that are present depending on cellular context and costimulatory signals (Chen et al., 1998b; Giffin et al., 2003; Jain et al., 1993; Molkentin et al., 1998; Stroud and Chen, 2003; Wu et al., 2006; Youn et al., 2000). This cooperation often occurs at composite elements containing adjacent binding sites of NFAT and its partners.

Initial speculation that NFAT may be involved in HIV-1 regulation came from the identification of putative NFAT binding sites on the HIV-1 LTR upstream of the tandem κB sites (Gaynor, 1992; Shaw et al., 1988). However, subsequent analyses concluded that no activity dependent on NFAT could be correlated with the presence of these motifs (Lu et al., 1990; Markovitz et al., 1992). Further studies reveal that the *cis* elements on the HIV-1 LTR recognized by NFAT are actually located in the

same enhancer region (nucleotides −104 to −80) recognized by NF-κB (Cron et al., 2000; Kinoshita et al., 1997). Meanwhile, evidence has also emerged that NFAT can activate transcription from κB-like sequences on a number of host and viral promoters (Goldfeld et al., 1993; Manley et al., 2006, 2008; Okamoto et al., 1994). Numerous studies now suggest that HIV-1 exploits NFAT for viral replication (Cron et al., 2000; Fortin et al., 2001; Kinoshita et al., 1997, 1998; Navarro et al., 1998). Induction of NFAT proteins has been shown to promote HIV-1 infection in primary $CD4^+$ cells, whereas inhibition of NFAT with the immunosuppressive drugs, CsA or FK506, suppresses this process (Argyropoulos and Mouzaki, 2006). Although CsA may act on multiple steps of the HIV-1 life cycle (Franke et al., 1994; Luban et al., 1993; Thali et al., 1994), significant evidence suggests that the inhibition of HIV-1 replication by CsA and FK506 is at least partly due to the inactivation of NFAT's transcriptional function (Cron, 2001; Cron et al., 2000; Kinoshita et al., 1997). Footprinting data indicate that NFAT binds to the tandem κB sites on the HIV-1 LTR (Cron et al., 2000; Kinoshita et al., 1997; Ranjbar et al., 2006). NFAT can activate reporter genes driven by the HIV-1 LTR, which requires the intact κB elements (Cron et al., 2000; Kinoshita et al., 1997). Interestingly, mutations of the spacer region between the two κB sites also disrupt the transcription function of the HIV-1 LTR (Kinoshita et al., 1997; Perkins et al., 1994), suggesting that the spacer binds additional factors or plays a role in coordinating the function of the two κB sites. Numerous studies also suggest that HIV-1 can induce cellular programs to promote viral replication. One prominent consequence of these cellular programs is the increased expression and activity of NFAT (Cicala et al., 2006). Taken together, these data strongly suggest that members of the NFAT family are involved in HIV-1 replication, but direct evidence has yet to come. It is interesting to speculate that the tandem κB sites and their linker region may have evolved to optimally exploit two different but related host factors (NF-κB and NFAT) for HIV-1 replication under different cellular conditions.

To aid further functional studies of NFAT in HIV-1 transcription and replication, we have been carrying out systematic structural studies of NFAT bound to the HIV-1 LTR. We have previously characterized the structure of NFAT bound to a single HIV-1 LTR κB site as a dimer (Giffin et al., 2003). Here, we present the crystal structure of the DNA binding domain of NFAT bound to the HIV-1 LTR tandem κB enhancer element as a higher-order complex. Our structure and accompanying biochemical analyses suggest that the binding of NFAT to Core I is affected by the nearby NFAT dimer bound to Core II. As a result, NFAT binds the two identical κB sites on the HIV-1 LTR in distinct modes. This observation may have general implications for DNA recognition by transcription factors in distinct promoter contexts in vivo. The DNA shows a significant bend near the 5′ end of Core I, where a lysine residue from NFAT bound to the 3′ end of Core II inserts into the minor groove. The insertion of the lysine residue also seems to cause two DNA bases to flip out toward the major groove, as suggested by the extra helical electron density observed in our crystal structure. These structural features of DNA distortion are consistent with in vivo footprinting data, and suggest that context-dependent DNA recognition by NFAT also involve conformational changes of DNA. Our structural and biochemical studies presented here have general implications for understanding the combinatorial mechanism of eukaryotic gene regulation and how this mechanism may be adopted by viruses in using host transcription machineries for viral replication.

RESULTS

Overview of the Structure

We have crystallized the RHR of human NFAT1 (amino acid residues 392–678) bound to a 25-mer double-stranded DNA containing the tandem κB sites from the HIV-1 LTR. The crystals diffracted to 3.05 Å resolution. The structure was solved by the molecular replacement method using the coordinates of NFAT1 bound to the isolated HIV-1 LTR κB site as a dimer (Giffin et al., 2003). The statistics of data collection and refinement are presented in Table S1 in the Supplemental Data available with this article online. The asymmetric unit of the crystal contains three molecules of NFAT bound to the HIV-1 LTR DNA (Figure 1), two of which form a dimer that binds one of the κB sites, whereas the third NFAT molecule binds the 3′ half site of the other κB site as a monomer. We have also crystallized a complex of NFAT bound to the HIV-1 LTR tandem κB sites on a 26-mer DNA and obtained a nearly identical structure, although at lower resolution (~3.5 Å) (D.L.B. and L.C., unpublished data). In the lattice of both the 25-mer and 26-mer structures, the NFAT monomer is surrounded by neighboring molecules, and there is no room for an additional NFAT molecule. But this does not necessarily mean that the observed 3:1 binding ratio is due to crystal packing. Nevertheless, biochemical verification of the binding stoichiometry in solution is needed (see below). The RHR of each NFAT molecule consists of two independently folded Ig domains, RHR-N and RHR-C; each resembles previously determined crystal structures in various NFAT complexes (Chen et al., 1998b; Giffin et al., 2003; Stroud and Chen, 2003; Wu et al., 2006). The DNA has a significant bend (about 35°) in the spacer region separating the two κB sites (discussed further below). Overall, NFAT binds the HIV-1 LTR tandem κB enhancer element as a mix of monomer and dimer.

Determining the Orientation of DNA

Since NFAT binds the two κB sites in very different modes, it is important to determine which site binds the NFAT dimer and which binds the monomer, or if the orientation of DNA is scrambled in the crystal lattice. In our previous study of the NFAT dimer bound to the HIV-1 LTR κB site, we used a 15-mer double-stranded DNA containing Core I and its flanking sequences (AATGGGGACTTTCCA) (Giffin et al., 2003). We used this structure as a partial search model to locate the NFAT dimer in the present crystal structure and initially assigned its DNA site as Core I. The electron density of DNA is very well defined (see below), although it is difficult to define the nucleotide sequence at 3.05 Å resolution. To determine the orientation of DNA in the crystal structure, we substituted Thy8 (Figure 1A, see sequence at bottom) in Core II with a 5-BrdU analog in the 25-mer DNA used in crystallization. The NFAT complex made with the modified DNA crystallized similarly to the native complex, and diffracted to 3.5 Å. We solved this structure by the molecular replacement method. A Fourier difference map shows clearly that the BrdU analog is located in the region where NFAT binds DNA as a dimer (Figure 2), whereas the corresponding site of the monomer lacks the extra density. This result demonstrates unambiguously that

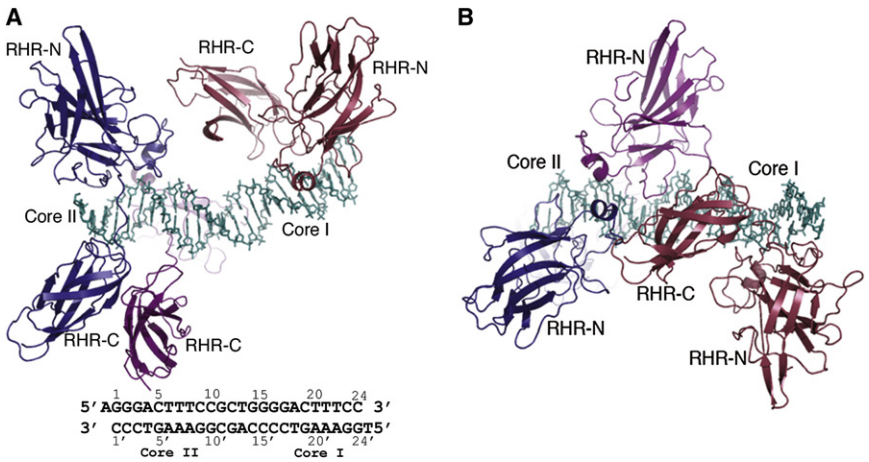

Figure 1. Overall Structure of the NFAT/HIV-1 LTR Tandem κB Complex

(A) The RHR of three NFAT molecules bind to the tandem κB sites of the HIV-1 LTR. The proteins are in ribbon style; the DNA is represented by the stick model (deep cyan). The NFAT monomer bound to the 3′ end of Core I is colored ruby red, and the NFAT dimer bound to Core II is colored deep purple (3′ end) and deep blue (5′ end). The N-terminal Ig domain (RHR-N) and the C-terminal Ig domain (RHR-C) are labeled for all three molecules. The DNA sequence used in the crystallization is listed at the bottom. Core I is from Gua15 to Cyt24, whereas Core II is from Gua1 to Cyt10. (B) The complex is rotated along the DNA axis by 90° with respect to (A).

DNA has a defined orientation in the crystal and that NFAT binds Core II as a dimer, while the third NFAT molecule binds the 3′ end of Core I as a monomer.

Two Distinct Conformations of NFAT on DNA

The NFAT monomer bound to the 3′ half of Core I adopts a V-shaped conformation. A number of residues from RHR-C engage in van der Waals interactions with residues from RHR-N. The linker region between RHR-N and RHR-C forms an α helix. These structural features are characteristic of the folded conformation of the NFAT RHR observed in a number of NFAT complexes characterized previously (Chen et al., 1998b; Giffin et al., 2003; Stroud and Chen, 2003; Wu et al., 2006). Indeed, the structure of the NFAT monomer on the HIV-1 LTR superimposes very well with the NFAT structure in the NFAT/Fos-Jun/DNA complex (Chen et al., 1998b; Figure 3A). In contrast to the NFAT monomer on Core I, the two NFAT molecules bound to Core II adopt an open conformation, wherein the linker between RHR-N and RHR-C assumes an extended conformation. There is no interaction between RHR-N and RHR-C. Instead, the RHR-C domains of both NFAT molecules interact with each other extensively to form the major dimer interface (discussed further below). The RHR-N also forms a small dimer interface through the E′F loop. The overall structure of the NFAT dimer bound to Core II is very similar to that observed in the NFAT dimer bound to an isolated HIV-1 LTR κB site (Giffin et al., 2003; Figure 3B). Thus, NFAT binds the HIV-1 LTR tandem κB sites in two distinct conformations, each representing a typical structure of NFAT RHR observed previously.

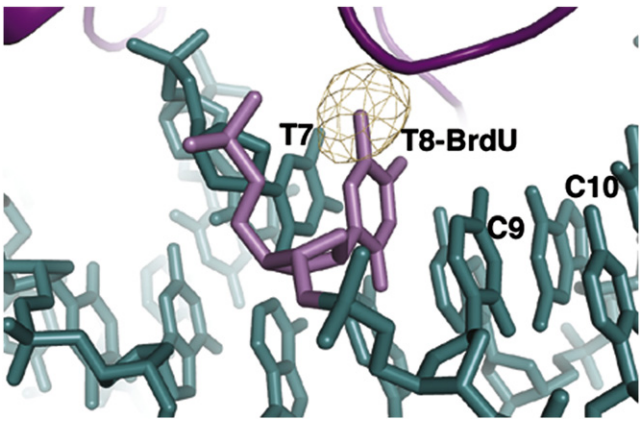

Figure 2. Orientation of the HIV-1 LTR Tandem κB DNA in the Crystal

A 5-BrdU base analog is engineered at the Thy8 position (magenta) in Core II. The Fourier difference map (contour level 3σ) shows clearly the extra density (yellow) corresponding to the heavier bromine atom. This region of DNA is occupied by the NFAT dimer.

DNA Conformation

A simulated-omit map shows that the refined DNA in the crystal structure has well-defined electron density (Figure 4A). Despite the application of B-DNA constraints during the refinement, the electron density shows that the middle region of the DNA is clearly bent from ideal B-DNA. Superposition of the DNA with an idealized B-DNA of the same sequence shows a 35° bend in the spacer region between the two κB sites (Figure 4B). The center of the bend is located near the 5′ end of Core I. Here, the major groove of DNA from Gua14 to Gua17 becomes widened, whereas the minor groove becomes narrowed. As discussed below, NFAT binding may contribute to or facilitate the DNA bend observed here. But we cannot rule out that HIV-1 LTR has an intrinsic tendency to bend between the two tandem κB sites.

Protein-Protein Interactions

Protein-protein interactions in the NFAT/HIV-1 LTR complex occur primarily between the two NFAT molecules bound to Core II. The RHR-C domains of both molecules interact with each other extensively to form a major dimer interface. On the other side of the DNA, the RHR-N domains also make contacts with each other, albeit to a lesser degree. As a result, the two NFAT molecules form a closed dimer that encircles the DNA (Figure 5A). The dimer interface formed by the RHR-C domains is asymmetric, involving strands *gaa′be* of one monomer and strands *fgcc′* of the other. The dimerization is mediated by extensive van der Waals contacts and hydrogen bonds between the main chain and side chain atoms of interface residues. Overall, the detailed dimerization interactions between the two NFAT molecules bound to Core II are very similar to those observed in the NFAT dimer bound to the isolated κB site (Giffin et al., 2003; Jin et al., 2003). Finally, the RHR-C of the NFAT monomer on Core I makes a small

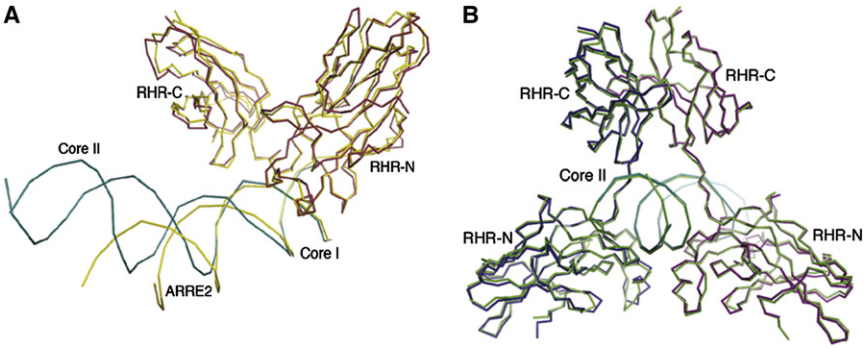

Figure 3. Two Distinct Conformations of the NFAT RHR on the HIV-1 LTR Tandem κB Sites

(A) Superposition of the NFAT monomer on the HIV-1 LTR Core I (protein, ruby red; DNA, dark cyan) and the NFAT monomer in the NFAT/Fos-Jun/ARRE2 complex (yellow). The Fos-Jun complex and the NFAT dimer on Core II are omitted for clarity. It is clear that the NFAT has a very similar structure in the two distinct complexes, including the relative orientation of the RHR-N and RHR-C. However, the DNA in the HIV-1 LTR complex (dark cyan) has a greater bend than that in the NFAT/Fos-Jun/ARRE2 complex (yellow) (discussed further in the text).

(B) Superposition of the NFAT dimer bound to Core II of the HIV-1 LTR tandem κB sites (dark blue) and the NFAT dimer bound to an isolated κB site (green). Both the protein and DNA superimpose very well in this region. The NFAT monomer bound to Core I is omitted.

contact to the RHR-N of the NFAT molecule bound to the 5′ end of Core II (Figure 5B).

Protein-DNA Interactions

The three NFAT molecules bind the HIV-1 LTR tandem κB sites through extensive interactions in the major and minor grooves and on the phosphate backbone. DNA recognition by NFAT is primarily mediated by a set of conserved structural elements in the RHR-N (Chen et al., 1998b). These elements include the AB loop and the RHR-N/RHR-C linker that interact with DNA bases in the major groove to specify the NFAT core sequence (GGAA) and the E′F loop that contacts the DNA backbone and minor groove. This general mode of DNA binding is largely conserved in the present structure. For the NFAT monomer bound to the 3′ end of Core I, Arg430, Arg421, Gln571, Glu427, and Tyr424 bind the major groove of DNA from Cyt19 to Cyt24. The stem of the E′F loop and the fg loop also make numerous contacts to the DNA backbone. Most notably, Arg537 inserts deeply into the minor groove (Figure 6). The NFAT molecule bound to the 3′ end of Core II interacts similarly with DNA from Cyt5 to Cyt10. The 5′ end of Core II contains a cryptic NFAT site (GGGA) instead of the consensus sequence (GGAA). On the consensus NFAT site, Arg430, Arg421, and Gln571 of NFAT form a stack of bidentate hydrogen bonds with the GGA trinucleotide motif. However, on the cryptic site of Core II, Arg430 and Arg421 form bidentate hydrogen bonds with Gua1 and Gua2, respectively, while the side chain of Gln571 forms only a single hydrogen bond with Gua3 (Figure 6). The detailed protein-DNA interactions on Core II are similar to those observed in the NFAT dimer bound to the isolated κB site (Giffin et al., 2003). In the present study, we also observed a novel protein-DNA contact by NFAT not seen in previous NFAT/DNA complexes. Lys482, which is located on the XY loop of the NFAT molecule bound to the 3′ end of Core II, inserts deeply into the minor groove between Gua14 and Gua15. The precise location of this insertion at the DNA bend suggests that Lys482 facilitates DNA bending by introducing a positive charge in the DNA minor groove.

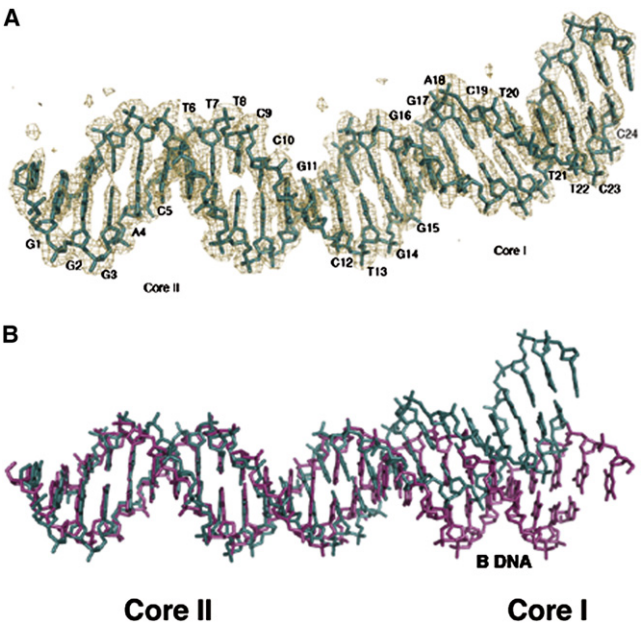

Figure 4. DNA conformation of the HIV-1 LTR tandem κB sites

(A) A simulated omit map (contour level 2σ) showing well-defined density of the HIV-1 LTR tandem κB sites and the distorted DNA helix. The sequence of the top strand is labeled.

(B) Superposition of the DNA in the crystal (dark cyan) and an ideal B-DNA containing the sequence of the HIV-1 LTR tandem κB sites (magenta) shows that the DNA bend is located at the 5′ end of Core I.

Biochemical Analyses of the NFAT/HIV-1 LTR Complex

Previous studies have shown that full-length NFAT1 and NFAT2 from cell extracts bind the HIV-1 LTR tandem κB sites as two major bands in the electrophoresis mobility shift assay (EMSA) gel (Cron et al., 2000). Since these two bands were not affected by mutations at the 5′ end of both κB sites, it was thought that NFAT binds at the 3′ end of the tandem κB sites as two independent monomers (Cron et al., 2000). We used highly purified NFAT1 RHR to observe a similar EMSA pattern for the binding of NFAT1 to the HIV-1 LTR tandem κB sites (Figure 7, lanes 1–3). We also found that the binding was not affected qualitatively by mutations at the 5′ end of both κB sites (data not shown). However, this observation does not necessarily suggest that NFAT binds only to the 3′ end consensus NFAT motif of the two κB sites as a monomer, because both NFAT5 and NF-κB have previously been shown to bind DNA with only one consensus half site as a dimer (Chen et al., 1998a; Stroud et al., 2002). We have previously shown that NFAT1 binds the isolated HIV-1 LTR κB site

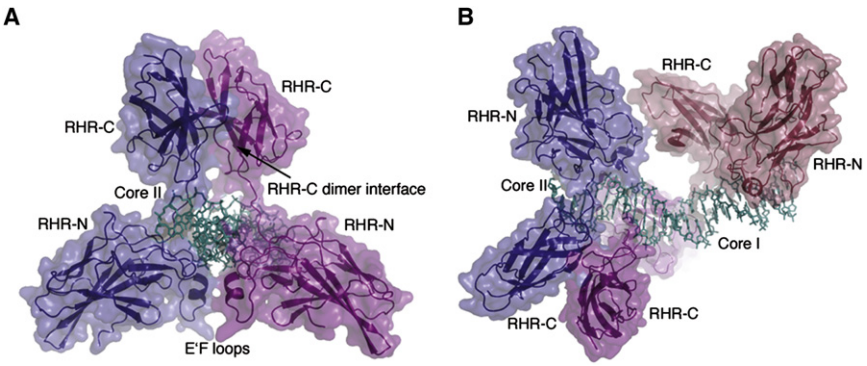

Figure 5. Protein-Protein Interactions in the NFAT/HIV-1 LTR Complex

(A) The NFAT dimer bound to Core II is shown in surface representation superimposed on the ribbon structure. The arrow indicates the major dimer interface formed by RHR-C. The E′F loop also makes a dimer interface on the opposite side of the DNA. As a result, DNA is encircled by the NFAT dimer. In this view, the NFAT monomer is omitted for clarity.

(B) Side view of the NFAT/HIV-1 LTR complex showing the small contact between the RHR-C of the NFAT monomer bound to Core I and the RHR-N of the NFAT molecule bound to the 5′ end of Core II. The DNA bend is also clearly visible, which may facilitate the interactions between NFAT molecules bound to Core I and Core II.

as a highly cooperative dimer (Giffin et al., 2003). Moreover, we found that NFAT can still bind 5′ end mutated HIV-1 LTR κB site as a dimer (Figure S1). Based on these observations and the present crystal structure, we favor the interpretation that the lower band in Figure 7 corresponds to one NFAT dimer bound to DNA, and the upper one corresponds to three NFAT molecules on DNA. Consistent with this interpretation, mutation at the 5′ end of Core I, which is unoccupied in the crystal structure, did not show any apparent effect on EMSA (Figure 7, lanes 4–6), but further mutation of the 3′ end consensus NFAT site of Core I eliminated the top band in EMSA, presumably by preventing the binding of the third NFAT molecule to Core I (Figure 7, lanes 7–9).

Since the molecular weight of protein-DNA complex on EMSA cannot be reliably predicted by its mobility, we further analyzed the binding stoichiometry by isothermal titration calorimetry (ITC). We used the isolated HIV-1 LTR κB site (AATGGGGAC TTTCCA) as a control to reliably obtain a titration ratio of 2:1 between NFAT1 and DNA (data not shown), which is consistent with the crystal structure (Giffin et al., 2003). However, on the HIV-1 tandem κB sites with various flanking sequences, the binding ratio between NFAT1 RHR and the DNA measured by ITC fluctuates between 2 and 3, and shows large error. A typical ITC run is shown in Figure 8. This behavior of binding ratio uncertainty was also observed in filter binding assays, which gave a stoichiometry of about 2.3–2.8. So far, we have been unable to determine the source of this apparent problem. One possibility is that the NFAT monomer binds the deformed Core I site with such weak affinity that the titration was not completed under our experimental conditions. In the crystal structure, the NFAT1 monomer bound to Core I indeed showed much higher B factors than the NFAT1 dimer bound to Core II. The NFAT/HIV-1 LTR complex is not stable enough for molecular weight analysis by gel filtration and multiangle light scattering. Chemical cross-linking of the NFAT/HIV-1 LTR complex and subsequent mass spectroscopy analyses revealed NFAT trimer, but also higher-order oligomers (M.J.G., D.L.B., and L.C., unpublished data).

To further address the question of whether the binding of NFAT1 to Core I is affected by the nearby Core II and/or the bound NFAT1 dimer, we inserted four bases between the two κB sites and compared the binding of NFAT1 RHR to the wild-type (WT) HIV-1 LTR DNA and the insertion mutant (insert mutant) (Figure 9). The inserted bases were added to the flanking

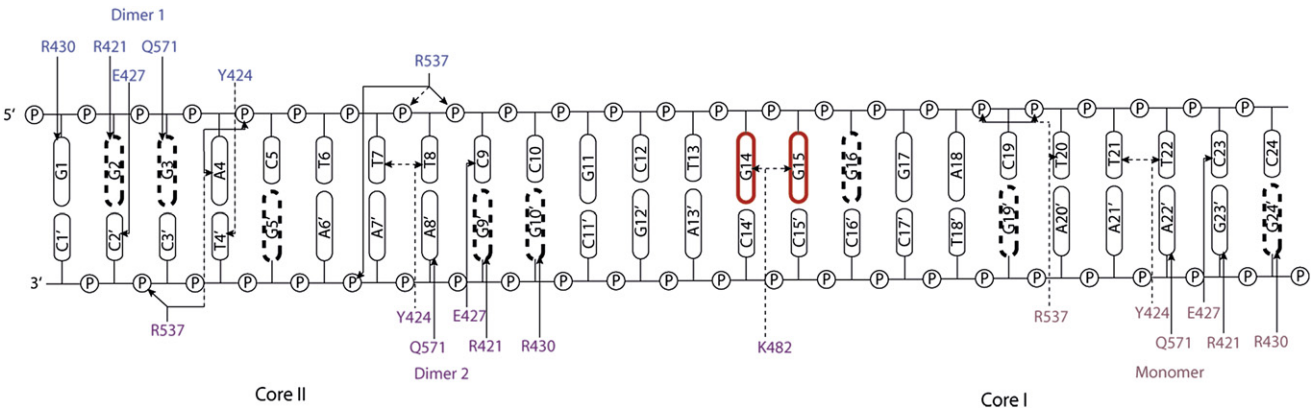

Figure 6. Schematic of Interactions between NFAT and the HIV-1 LTR Tandem κB Sites

DNA is represented as a ladder, with bases as ovals and labeled according to the text and Figure 1A. The backbone phosphates are represented as circles, with the letter P inside. "Monomer" represents the NFAT molecule bound to the 3′ end of Core I, the residues of which are colored ruby red. "Dimer 2" represents the NFAT molecule bound to the 3′ end of Core II, the residues of which are colored deep purple. "Dimer 1" represents the NFAT molecule bound to the 5′ end of Core II, the residues of which are colored deep blue. Hydrogen bonding interactions are represented by solid arrows, while van der Waals interactions are represented by dashed arrows. The guanine nucleotides protected in the in vivo DMS footprinting are highlighted by bold, dashed ellipses, whereas guanine residues with enhanced reactivity toward DMS are highlighted by bold, red ellipses. For clarity, only representative protein-DNA contacts are shown in the figure.

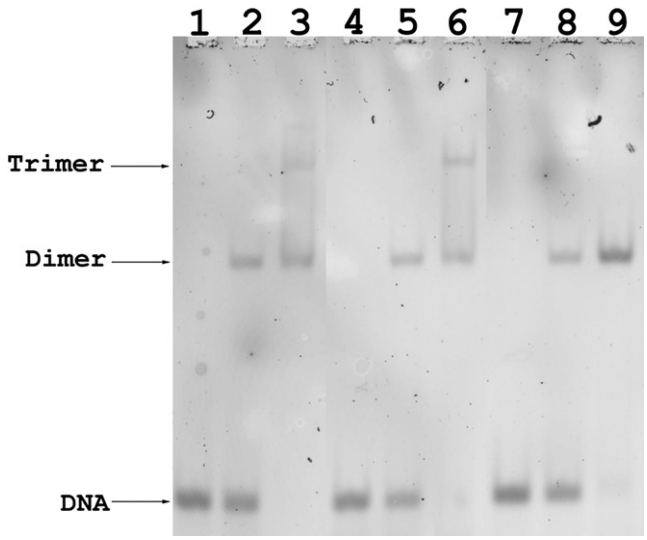

Figure 7. EMSA of NFAT1 RHR Binding to the HIV-1 LTR Tandem κB Sites

DNA containing the WT HIV-1 LTR tandem κB sequences (lanes 1–3), the mutant modified at the 5′ end of Core I (lanes 4–6), or the mutant modified at both the 5′ and 3′ ends of Core I (lanes 7–9) are used in three sets of binding reactions. The detailed sequence changes in both mutants are described in Experimental Procedures. The DNA concentration was kept at 1 nM. For each set of DNA (lanes 1–3, lanes 4–6, or lanes 7–9), the concentration of NFAT RHR varies between 0, 4, and 40 nM. DNA = unbound free DNA; Dimer = two NFAT molecules bound to DNA; Trimer = three NFAT molecules bound to DNA.

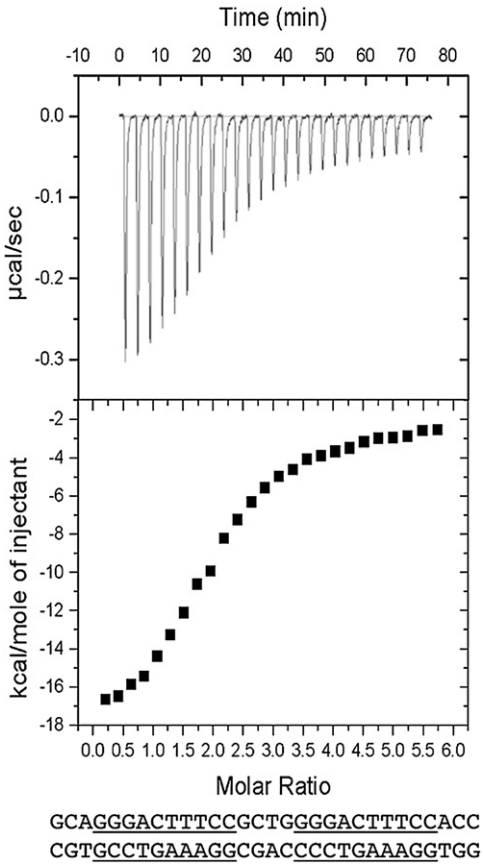

Figure 8. ITC Analysis of NFAT1 RHR Binding to the HIV-1 LTR Tandem κB Sites

The top panel presents heat effects associated with the injection of DNA into the solution of NFAT1 RHR. The bottom panel presents DNA concentration dependence of the heat released upon DNA binding to NFAT1 after normalization and correction for the heats of dilution. The horizontal axis represents the NFAT versus DNA molar ratio. The DNA sequence used in this experiment is at the bottom (see Experimental Procedures for further details).

region of the WT probe to make the length equal. Titration of the WT HIV-1 LTR DNA with NFAT1 RHR (Figure 9A, lanes 1–6) showed two major bands, as seen in Figure 7. However, with high concentration of DNA probe and longer exposure here, we also observed a minor band between the two major bands. The identity of this minor band is not clear, but probably corresponds to a different intermediate other than the NFAT1 dimer bound to Core II before the fully titrated complex is formed (Figure 9A, lane 6). Titration of the insert mutant (Figure 9A, lanes 7–12) also generated two bands. Our previous biochemical and structural studies have demonstrated that NFAT1 RHR can bind isolated Ig κB sites in various DNA contexts as a highly cooperative dimer (Giffin et al., 2003; Jin et al., 2003). We can therefore reasonably assign the lower band as the dimer and the higher band as two dimers on the insert mutant. The formation of the two dimers on the insert mutant seems to be noncooperative, suggesting that the binding of NFAT to the two further separated κB sites are independent. We can use the bands of the insert mutant as calibration to see that the lower band formed on the WT probe has the same mobility as that of the insert mutant (Figure 9A, compare lanes 2–4 and 8–10), whereas the higher band has a slightly faster mobility than the corresponding band of the insert mutant (Figure 9A, compare lanes 6 and 12). We have also stained the gel for DNA (Figure 9A) and protein (Figure 9B), and analyzed the band intensity by densitometry. Although we could not obtain a quantitative measurement of the binding stoichiometry by this method, we observed reproducibly that the protein:DNA ratio for the lower band is significantly less than that for the higher band on the WT probe, and that the protein:DNA ratio of the higher band formed on the WT probe is significantly less than that of the higher band formed on the insert mutant (Figure 9B, compare lanes 6 and 12). These observations are consistent with the interpretation that the lower and higher bands on the WT probe correspond to 2:1 and 3:1 complexes, whereas those on the insert mutant correspond to the 2:1 and 4:1 complexes.

Comparison with In Vivo Footprinting Data

Protein binding to the HIV-1 LTR has been analyzed by in vivo dimethylsulfate (DMS) footprinting, which reveals potential protein contacts under physiological conditions (Demarchi et al., 1992, 1993). In these studies, HIV-1-infected T cells were treated with DMS. The resulting footprinting pattern revealed extensive protection of guanine nucleotides in both the Core II and Core I regions, including Gua2, Gua3, Gua5′, Gua9′, Gua10′, Gua16, Gua19′, and Gua24′ (Figure 6). Most of the protected guanines, such as Gua2, Gua3, Gua9′, Gua10′, and Gua24′, are contacted by NFAT in our crystal structure, but some of them (Gua5′, Gua16, and Gua19′) are apparently open to solvent. Protection of these guanines might arise from the binding of other factors in vivo. Alternatively, full-length NFAT may make additional

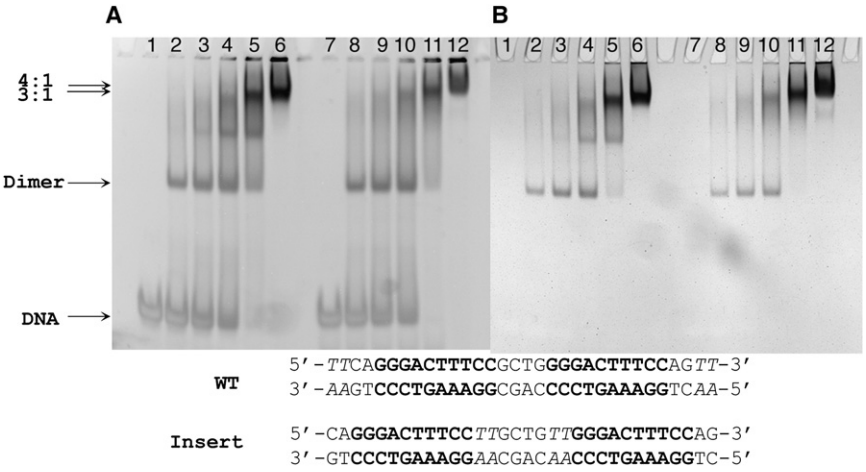

Figure 9. Effect of the Spacing between the Two κB Sites in the HIV-1 LTR

(A) EMSA of NFAT1 RHR binding to the WT HIV-1 LTR (WT) (lanes 1–6) or the insert mutant (lanes 7–12). The sequences of both probes are listed below the gel, with the inserted bases italicized. The DNA was kept at 0.1 nmol. For each set of DNA probe (lanes 1–6 or lanes 7–12), the molar ratio of protein (NFAT RHR) to DNA varies between 0, 0.5, 1, 2, 4, and 6. The gel was stained for DNA.

(B) The same gel was stained for protein.

contacts to the HIV-1 LTR DNA through domains that are not included in the current crystal structure. Interestingly, upon transcriptional activation, the most significant change in the footprinting pattern is a dramatic increase in DMS reactivity of Gua14 and Gua15 in the spacer region between the two κB sites (Demarchi et al., 1993). Our structure reveals a 35° DNA bend around Gua14 and Gua15, where Lys482 (see above) interacts with the two guanines in the minor groove. A simulated omit map of this region of DNA reveals extra helical density around Gua14 and Gua15 (Figure 10), suggesting that Gua14 or Gua15, or both, have a tendency to flip out the DNA helix, probably due to the DNA bend and/or the insertion of Lys482 in the minor groove. These structural features may explain the enhanced reactivity of the two guanines toward DMS. These observations, together with the partial agreement of guanine protection, hint that NFAT might bind the HIV-1 LTR tandem κB sites in vivo in a structure similar to that observed here.

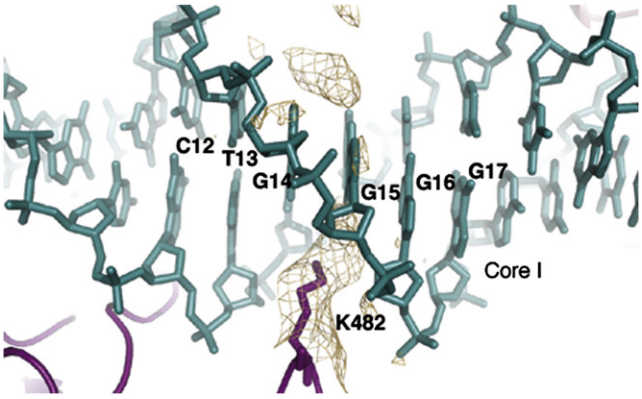

Figure 10. Detailed View of the DNA Bending Region

A simulated omit map (contour level 3σ) showing well-defined density of Lys482 of the NFAT molecule bound to the 3′ end of Core II. This lysine residue inserts deeply into the minor groove opposing Gua14 and Gua15. Although, at the current resolution, the exact conformation of individual bases cannot be refined without B-DNA constraints, a pronounced density is observed in the major groove of Gua14 and Gua15, suggesting that these two bases are distorted, perhaps becoming extrahelical. These two bases showed enhanced reactivity toward DMS in the in vivo footprinting (see text for further details).

DISCUSSION

Although many cellular promoters contain multiple κB sites, the specific configuration of the tandem κB sites conserved on the HIV-1 LTR has not been found in any known host promoters (M. Hartwig and L.C., unpublished data). This observation raises an intriguing question if the NFAT or the NF-κB complexes formed on the HIV-1 LTR are structurally unique and, therefore, may be selectively inhibited by small molecules. Based on the structure of NFAT dimer bound to the isolated HIV-1 LTR κB site (Giffin et al., 2003), we built a model of NFAT bound to the HIV-1 LTR tandem κB sites (Figure S2). The model suggests that the two NFAT dimers bound to the adjacent κB sites would clash with each other, which may explain why NFAT binds the HIV-1 LTR tandem κB sites as a mix of monomer and dimer. There is little protein-protein interaction between the NFAT dimer bound to Core II and the NFAT monomer on Core I. Consistent with this assembly, EMSA and filter binding assays show that NFAT binds the HIV-1 κB site as a cooperative dimer (Hill coefficient, 1.85), but the binding of the additional NFAT molecule seems noncooperative (Hill coefficient for the tandem κB sites, 1.87) (M.J.G. and L.C., unpublished data). However, inside cells, full-length NFAT bound to Core I and Core II may interact with each other through regions outside RHR. The three NFAT molecules on the HIV-1 LTR may, therefore, act together to recruit transcription coactivators to drive HIV-1 transcription.

The tandem κB sites on the HIV-1 LTR have identical core sequences (GGGACTTTCC). It is, therefore, intriguing that NFAT binds these two sites in such drastically different modes. The main differences between the two sites are the immediate flanking sequences and their relative arrangement on DNA (i.e., Core I is located on the 5′ side of Core II reading from the coding strand). Our previous studies have shown that NFAT can bind the isolated Core I with its native flanking sequences (TGGGGACTTTCCA) as a cooperative dimer (Giffin et al., 2003). Thus, the immediate flanking sequences are unlikely the cause of the difference. The HIV-1 LTR tandem κB sites have a severe bend near the 5′ end of Core I, which may prevent the binding of NFAT to this site. This DNA bend is apparently facilitated by Lys482 from the NFAT molecule bound to the 3′ end of Core II. Why does NFAT not bind Core I as a dimer and induce a bend at the 3′ end of Core II so that Core II binds an NFAT monomer? It is possible that the 5′ end of Core I in the HIV-1 LTR has an intrinsic bend or has a high propensity to bend as compared with the 3′ end of Core II. The asymmetric nature of the spacer sequences

(coding strand GCTG, noncoding strand CAGC) may partially account for this difference. Thus, the function of a *cis*-regulatory element may be affected by the flanking DNA sequences and proximal cofactors. These observations have general implications for understanding the allosteric effect of DNA and the combinatorial mechanism of eukaryotic gene regulation (Lefstin and Yamamoto, 1998; Yamamoto et al., 1992).

Structural analyses of various NFAT/DNA complexes have so far revealed two major conformations of NFAT RHR on DNA. In the NFAT/Fos-Jun/DNA complex and the NFAT/FOXP2/DNA complex (Chen et al., 1998b; Wu et al., 2006), the RHR of NFAT assumes a fold-up structure, wherein RHR-N and RHR-C interact with each other and with other transcription factor partners. In the NFAT dimer bound to the κB site (Giffin et al., 2003; Jin et al., 2003), the RHR of NFAT adopts an extended conformation, wherein the RHR-C domains of each protein interact with each other to form the major dimer interface. Structural analyses of a NFAT monomer bound to the consensus NFAT site also reveal that the RHR of NFAT adopts one of these two conformations, even in the absence of interaction partners (Stroud and Chen, 2003). Here, we have observed the two representative conformations of NFAT in the same complex. These results suggest that the relative conformations of RHR-N and RHR-C are not completely flexible as initially thought (Chen et al., 1998b), but, rather, have a high propensity to adopt one of two distinct conformations. This conclusion has important implications for understanding the interaction between NFAT and other transcription factors on composite sites. For example, in the NFAT/Fos-Jun/DNA complex, RHR-C makes a contact to Fos (Chen et al., 1998b). In the NFAT/FOXP2/DNA complex, RHR-N and RHR-C fold up to form a groove into which the wing1 of FOXP2 inserts (Wu et al., 2006). All these interactions are unlikely incidental contacts induced by crystal packing that locks the RHR-C position, but, rather, represent functional interactions intrinsic to NFAT.

The dimer interface formed by the RHR-C of NFAT differs significantly from the classical rel dimer interface observed in NF-κB (Ghosh et al., 1995; Muller et al., 1995). The interface is asymmetric and highly hydrophilic, atypical of protein-protein interfaces seen in many stable protein complexes. This structural feature is consistent with the fact that NFAT does not form a stable dimer without binding to DNA. In the present study, the two NFAT molecules bound to Core II show identical protein-protein interactions with those observed in previous studies, providing further support for the unusual mode of dimerization observed in NFAT. Our previous study of the NFAT dimer bound to the isolated HIV-1 LTR κB site reveals that NFAT encircles the DNA through two dimer interfaces, one formed by the RHR-C, and the other by the RHR-N (Giffin et al., 2003). By contrast, the NFAT dimer bound to a κB site from the IL-8 promoter adopts an open conformation, wherein only the RHR-C dimer interface is formed (Jin et al., 2003). Based on the DNA interaction details, we have proposed a mechanism by which subtle nucleotide sequence variations in the κB site can induce a large conformation change in NFAT (Giffin et al., 2003). Although this model is consistent with the observations that κB sites with single nucleotide differences can confer distinct functions in vivo (Leung et al., 2004), we cannot rule out the possibility that the closed conformation of the NFAT dimer is caused by crystal packing (Giffin et al., 2003). Here, on the tandem κB sites and in a very different crystal packing environment, the NFAT dimer bound to Core II is nearly identical to the previously observed structure (Figure 5). This observation strongly suggests that the closed conformation of the NFAT dimer on the HIV-1 LTR is a result of binding to the specific κB sequences.

NFAT binds the HIV-1 LTR tandem κB sites following the general model of DNA recognition by NFAT previously defined in a series of NFAT/DNA complexes (Chen et al., 1998b; Giffin et al., 2003; Jin et al., 2003; Stroud and Chen, 2003; Wu et al., 2006). Namely, a set of highly conserved residues (Arg430, Arg421, and Gln571) from the AB loop and the RHR-N/RHR-C linker bind the consensus GGA sequence or the cryptic GGG sequence. The XY loop of the RHR has been predicted to bind DNA based on the structure of NF-κB (Muller et al., 1995). Indeed, as observed here on the longer DNA of the HIV-1 LTR tandem κB sites, Lys482 from the XY loop of the RHR-N inserts in the minor groove of the spacer region. This observation suggests that flanking sequences outside the consensus site (GGAA) may affect NFAT binding and its transcription functions, and that NFAT may affect protein-DNA interactions and DNA structure far beyond its core binding site.

Our structure is consistent with a large body of biochemical data on the HIV-1 LTR. Mutations in the κB sites have been shown to diminish the transcription function of the HIV-1 LTR in reporter assays (Cron et al., 2000; Kinoshita et al., 1997). In our structure, these mutations correspond to bases that make critical contacts to NFAT. Interestingly, mutations of the spacer region have also been shown to disrupt the function of the HIV-1 LTR (Kinoshita et al., 1997; Perkins et al., 1994). This result was interpreted as indicating another factor binding to the spacer region (Perkins et al., 1994). Our structure suggests that the spacer region, together with the unoccupied 5′ end of Core I, may accommodate another factor. Alternatively, mutations in the spacer region may alter the DNA bend and, hence, disrupt the function of the HIV-1 LTR. Most strikingly, the DNA structure distortion observed in our crystal structure matches exactly with the DMS hypersensitivity in in vivo footprinting (Demarchi et al., 1993). Nevertheless, additional work is necessary to determine the functional relevance of this structure. Our structural and biochemical studies presented here will provide a molecular framework for further exploration of the regulatory mechanisms of HIV-1 transcription and replication.

EXPERIMENTAL PROCEDURES

Sample Preparation and Crystallization

Recombinant human NFAT1 (392–678, with an 18 residue N-terminal His-tag) was expressed and purified as previously described (Chen et al., 1998b). DNA oligonucleotides were purchased from Integrated DNA Technologies and purified by Mono Q column (Pharmacia). The NFAT1-DNA complex was prepared by mixing 4:1 equivalents of NFAT1 and DNA at a concentration of 0.1–0.2 mM in a dilution buffer containing 10 mM HEPES (pH 7.5), 100 mM NaCl, 8% (v/v) glycerol, and 350 mM NH_4OAc. Crystals of the NFAT1-DNA complex were grown at 18°C by the hanging-drop method with a reservoir buffer of 50 mM HEPES (pH 7.0), 15 mM magnesium acetate, 250 mM ammonium acetate, and 7.5% PEG4K. Typically, crystals grew to 200 × 70 × 70 μm in 1 wk. The crystals belong to the space group *P2*(1)2(1)2(1), with cell dimensions *a* = 93.691 Å, *b* = 95.299 Å, and *c* = 159.227 Å.

Data Collection, Structure Determination, and Analysis

Crystals were stabilized in the harvest-cryoprotectant buffer: 10 mM HEPES (pH 7.0), 200 mM ammonium acetate, 15 mM magnesium acetate, 10%–12%

(w/v) PEG4K, and 25% (v/v) glycerol. All crystals were flash frozen in liquid nitrogen for storage and for data collection under cryogenic conditions (100 K). The native data were collected at the Advanced Photon Source (Argonne National Laboratory, Argonne, IL) beamline (14-BM-C, wavelength 0.9795 Å). Bromine data were collected at the Advanced Light Source (Lawrence Berkeley National Laboratory, Berkeley, CA) beamline (8.2.2, wavelength 0.9204 Å).

Data were reduced with HKL2000 (Otwinowski and Minor, 1997). The structure of the NFAT1-DNA complex was solved by the molecular replacement method, with the dimer of NFAT1 from NFAT1 bound as a dimer to the HIV-1 LTR element as a partial search model (Giffin et al., 2003). Refinement, model building, and analysis were carried out with CNS (Brunger et al., 1998) and O (Jones et al., 1991). Final models have very good geometry. All residues have backbone and angles in the "allowed" region of a Ramachandran plot, with 80% in the most favored region. The statistics of the crystallographic analysis are presented in Table S1. Figures illustrating structure were prepared with PyMOL (DeLano, 2002).

EMSA

The EMSA was performed in a buffer of 20 mM HEPES (pH 7.7), 100 mM NaCl, 1 mM DTT, and 10% glycerol, with various concentrations of the NFAT1 RHR and DNA containing the WT or modified HIV-1 LTR tandem κB sequences. For Figure 7, the WT sequence (5′-CAAGGGACTTTCCGCTGGGGACTTTCCAGG-3′ [κB sites underlined]) or the mutant modified at the 5′ end of Core I (5′-CAAGGGACTTTCCGCTG*ACA*ACTTTCCAGG-3′ [mutated bases italicized]), or the mutant modified at both the 5′ and 3′ ends of Core I (5′-CAAGGGACTTTCCGCTG*ACA*ACTTT*GT*AGG-3′ [mutated bases italicized]) were used. For all binding reactions, the DNA was kept at 1.0 nM, while the concentration of NFAT1 RHR varied between 0, 4, and 40 nM. The total reaction volume was 20 μl. In Figure 9, the sequences are listed below the gel and the concentration of DNA and protein are as indicated in the figure legend. The binding reactions were incubated at room temperature for 30 min and run on 5% native polyacrylamide gel in 0.5× TBE buffer. The gel was stained for DNA with SYBR safe DNA stain (Invitrogen) or for protein with Coomassie blue.

ITC Analysis

The ITC was carried out at 30°C with a MicroCal VP-ITC titration calorimeter (MicroCal, Inc). NFAT1 RHR (50 μM) in ITC buffer (10 mM HEPES [pH 7.5], 250 mM NaCl, 0.5 mM EDTA) was added to the sample cell (~1.45 ml), and a 200–500 μM solution of DNA titrant was loaded into the 293 μl injection syringe. Each titration consisted of a preliminary 3 μl injection, followed by 20–50 subsequent injections of 8–10 μl of DNA into the sample cells. To correct for dilution and mixing effects, a series of control injections was carried out, in which DNA was injected in buffer alone. The heat signal of this control was then subsequently subtracted from the raw data for each NFAT/DNA titration. The ITC data were analyzed with MicroCal ORIGIN software. The ITC data could not be fitted to a simple Langmuir model, indicating a complicated binding mode of NFAT to the HIV-1 tandem κB sites. The binding stoichiometry between NFAT and DNA obtained from ITC shows a large error and fluctuates between 2 and 3.

ACCESSION NUMBERS

Coordinates and structural factors have been deposited in the RCSB protein database under accession code 2O93.

SUPPLEMENTAL DATA

Supplemental Data include one table and two figures and are available with this article online at http://www.structure.org/cgi/content/full/16/5/684/DC1/.

ACKNOWLEDGMENTS

The authors thank Mark Hartwig and K.C. Wumesh for discussion and Steve Edwards for help in data collection. D.B., K.B., and J.C.S. have been supported by a National Institutes of Health (NIH) training grant. This research is supported by grants from the NIH (to L.C.).

Received: March 12, 2007
Revised: January 24, 2008
Accepted: January 24, 2008
Published: May 6, 2008

REFERENCES

Alcami, J., Lain de Lera, T., Folgueira, L., Pedraza, M.A., Jacque, J.M., Bachelerie, F., Noriega, A.R., Hay, R.T., Harrich, D., Gaynor, R.B., et al. (1995). Absolute dependence on κB responsive elements for initiation and Tat-mediated amplification of HIV transcription in blood CD4 T lymphocytes. EMBO J. *14*, 1552–1560.

Argyropoulos, C., and Mouzaki, A. (2006). Immunosuppressive drugs in HIV disease. Curr. Top. Med. Chem. *6*, 1769–1789.

Bounou, S., Dumais, N., and Tremblay, M.J. (2001). Attachment of human immunodeficiency virus-1 (HIV-1) particles bearing host-encoded B7–2 proteins leads to nuclear factor-κ B- and nuclear factor of activated T cells-dependent activation of HIV-1 long terminal repeat transcription. J. Biol. Chem. *276*, 6359–6369.

Brunger, A.T., Adams, P.D., Clore, G.M., DeLano, W.L., Gros, P., Grosse-Kunstleve, R.W., Jiang, J.S., Kuszewski, J., Nilges, M., Pannu, N.S., et al. (1998). Crystallography & NMR system: A new software suite for macromolecular structure determination. Acta Crystallogr. D Biol. Crystallogr. *54*, 905–921.

Chen, B.K., Feinberg, M.B., and Baltimore, D. (1997). The κB sites in the human immunodeficiency virus type 1 long terminal repeat enhance virus replication yet are not absolutely required for viral growth. J. Virol. *71*, 5495–5504.

Chen, Y.Q., Ghosh, S., and Ghosh, G. (1998a). A novel DNA recognition mode by the NF-κ B p65 homodimer. Nat. Struct. Biol. *5*, 67–73.

Chen, L., Glover, J.N., Hogan, P.G., Rao, A., and Harrison, S.C. (1998b). Structure of the DNA-binding domains from NFAT, Fos and Jun bound specifically to DNA. Nature *392*, 42–48.

Choi, J., Walker, J., Talbert-Slagle, K., Wright, P., Pober, J.S., and Alexander, L. (2005). Endothelial cells promote human immunodeficiency virus replication in nondividing memory T cells via Nef-, Vpr-, and T-cell receptor-dependent activation of NFAT. J. Virol. *79*, 11194–11204.

Cicala, C., Arthos, J., Selig, S.M., Dennis, G., Jr., Hosack, D.A., Van Ryk, D., Spangler, M.L., Steenbeke, T.D., Khazanie, P., Gupta, N., et al. (2002). HIV envelope induces a cascade of cell signals in non-proliferating target cells that favor virus replication. Proc. Natl. Acad. Sci. USA *99*, 9380–9385.

Cicala, C., Arthos, J., Censoplano, N., Cruz, C., Chung, E., Martinelli, E., Lempicki, R.A., Natarajan, V., VanRyk, D., Daucher, M., et al. (2006). HIV-1 gp120 induces NFAT nuclear translocation in resting CD4+ T-cells. Virology *345*, 105–114.

Crabtree, G.R., and Olson, E.N. (2002). NFAT signaling: choreographing the social lives of cells. Cell Suppl. *109*, S67–S79.

Cron, R.Q. (2001). HIV-1, NFAT, and cyclosporin: immunosuppression for the immunosuppressed? DNA Cell Biol. *20*, 761–767.

Cron, R.Q., Bartz, S.R., Clausell, A., Bort, S.J., Klebanoff, S.J., and Lewis, D.B. (2000). NFAT1 enhances HIV-1 gene expression in primary human CD4 T cells. Clin. Immunol. *94*, 179–191.

DeLano, W.L. (2002). The PyMOL Molecular Graphics System (Palo Alto, CA: DeLano Scientific).

Demarchi, F., D'Agaro, P., Falaschi, A., and Giacca, M. (1992). Probing protein-DNA interactions at the long terminal repeat of human immunodeficiency virus type 1 by in vivo footprinting. J. Virol. *66*, 2514–2518.

Demarchi, F., D'Agaro, P., Falaschi, A., and Giacca, M. (1993). In vivo footprinting analysis of constitutive and inducible protein-DNA interactions at the long terminal repeat of human immunodeficiency virus type 1. J. Virol. *67*, 7450–7460.

Fenard, D., Yonemoto, W., de Noronha, C., Cavrois, M., Williams, S.A., and Greene, W.C. (2005). Nef is physically recruited into the immunological synapse and potentiates T cell activation early after TCR engagement. J. Immunol. *175*, 6050–6057.

 ©2008 Elsevier Ltd All rights reserved

Fortin, J.F., Barbeau, B., Robichaud, G.A., Pare, M.E., Lemieux, A.M., and Tremblay, M.J. (2001). Regulation of nuclear factor of activated T cells by phosphotyrosyl-specific phosphatase activity: a positive effect on HIV-1 long terminal repeat-driven transcription and a possible implication of SHP-1. Blood *97*, 2390–2400.

Franke, E.K., Yuan, H.E., and Luban, J. (1994). Specific incorporation of cyclophilin A into HIV-1 virions. Nature *372*, 359–362.

Gaynor, R. (1992). Cellular transcription factors involved in the regulation of HIV-1 gene expression. AIDS *6*, 347–363.

Ghosh, G., van Duyne, G., Ghosh, S., and Sigler, P.B. (1995). Structure of NF-κB p50 homodimer bound to a κB site. Nature *373*, 303–310.

Giffin, M.J., Stroud, J.C., Bates, D.L., von Koenig, K.D., Hardin, J., and Chen, L. (2003). Structure of NFAT1 bound as a dimer to the HIV-1 LTR κB element. Nat. Struct. Biol. *10*, 800–806.

Goldfeld, A.E., McCaffrey, P.G., Strominger, J.L., and Rao, A. (1993). Identification of a novel cyclosporin-sensitive element in the human tumor necrosis factor α gene promoter. J. Exp. Med. *178*, 1365–1379.

Greene, W.C. (1990). Regulation of HIV-1 gene expression. Annu. Rev. Immunol. *8*, 453–475.

Hogan, P.G., Chen, L., Nardone, J., and Rao, A. (2003). Transcriptional regulation by calcium, calcineurin, and NFAT. Genes Dev. *17*, 2205–2232.

Jain, J., McCaffrey, P.G., Miner, Z., Kerppola, T.K., Lambert, J.N., Verdine, G.L., Curran, T., and Rao, A. (1993). The T-cell transcription factor NFATp is a substrate for calcineurin and interacts with Fos and Jun. Nature *365*, 352–355.

Jeeninga, R.E., Hoogenkamp, M., Armand-Ugon, M., de Baar, M., Verhoef, K., and Berkhout, B. (2000). Functional differences between the long terminal repeat transcriptional promoters of human immunodeficiency virus type 1 subtypes A through G. J. Virol. *74*, 3740–3751.

Jin, L., Sliz, P., Chen, L., Macian, F., Rao, A., Hogan, P.G., and Harrison, S.C. (2003). An asymmetric NFAT1 dimer on a pseudo-palindromic κB-like DNA site. Nat. Struct. Biol. *10*, 807–811.

Jones, T.A., Zou, J.Y., Cowan, S.W., and Kjeldgaard, M. (1991). Improved methods for building protein models in electron density maps and the location of errors in these models. Acta Crystallogr. A *47*, 110–119.

Kawakami, K., Scheidereit, C., and Roeder, R.G. (1988). Identification and purification of a human immunoglobulin-enhancer-binding protein (NF-κB) that activates transcription from a human immunodeficiency virus type 1 promoter in vitro. Proc. Natl. Acad. Sci. USA *85*, 4700–4704.

Kinoshita, S., Su, L., Amano, M., Timmerman, L.A., Kaneshima, H., and Nolan, G.P. (1997). The T cell activation factor NF-ATc positively regulates HIV-1 replication and gene expression in T cells. Immunity *6*, 235–244.

Kinoshita, S., Chen, B.K., Kaneshima, H., and Nolan, G.P. (1998). Host control of HIV-1 parasitism in T cells by the nuclear factor of activated T cells. Cell *95*, 595–604.

Lefstin, J.A., and Yamamoto, K.R. (1998). Allosteric effects of DNA on transcriptional regulators. Nature *392*, 885–888.

Leonard, J., Parrott, C., Buckler-White, A.J., Turner, W., Ross, E.K., Martin, M.A., and Rabson, A.B. (1989). The NF-κB binding sites in the human immunodeficiency virus type 1 long terminal repeat are not required for virus infectivity. J. Virol. *63*, 4919–4924.

Leung, T.H., Hoffmann, A., and Baltimore, D. (2004). One nucleotide in a κB site can determine cofactor specificity for NF-κB dimers. Cell *118*, 453–464.

Levine, B.L., Mosca, J.D., Riley, J.L., Carroll, R.G., Vahey, M.T., Jagodzinski, L.L., Wagner, K.F., Mayers, D.L., Burke, D.S., Weislow, O.S., et al. (1996). Antiviral effect and ex vivo $CD4^+$ T cell proliferation in HIV-positive patients as a result of CD28 costimulation. Science *272*, 1939–1943.

Lu, Y.C., Touzjian, N., Stenzel, M., Dorfman, T., Sodroski, J.G., and Haseltine, W.A. (1990). Identification of *cis*-acting repressive sequences within the negative regulatory element of human immunodeficiency virus type 1. J. Virol. *64*, 5226–5229.

Luban, J., Bossolt, K.L., Franke, E.K., Kalpana, G.V., and Goff, S.P. (1993). Human immunodeficiency virus type 1 Gag protein binds to cyclophilins A and B. Cell *73*, 1067–1078.

Manley, K., O'Hara, B.A., Gee, G.V., Simkevich, C.P., Sedivy, J.M., and Atwood, W.J. (2006). NFAT4 is required for JC virus infection of glial cells. J. Virol. *80*, 12079–12085.

Manley, K., O'Hara, B.A., and Atwood, W.J. (2008). Nuclear factor of activated T-cells (NFAT) plays a role in SV40 infection. Virology *372*, 48–55.

Markovitz, D.M., Hannibal, M.C., Smith, M.J., Cossman, R., and Nabel, G.J. (1992). Activation of the human immunodeficiency virus type 1 enhancer is not dependent on NFAT-1. J. Virol. *66*, 3961–3965.

McCaffrey, P.G., Luo, C., Kerppola, T.K., Jain, J., Badalian, T.M., Ho, A.M., Burgeon, E., Lane, W.S., Lambert, J.N., Curran, T., et al. (1993). Isolation of the cyclosporin-sensitive T cell transcription factor NFATp. Science *262*, 750–754.

Michael, N.L., Vahey, M., Burke, D.S., and Redfield, R.R. (1992). Viral DNA and mRNA expression correlate with the stage of human immunodeficiency virus (HIV) type 1 infection in humans: evidence for viral replication in all stages of HIV disease. J. Virol. *66*, 310–316.

Molkentin, J.D., Lu, J.R., Antos, C.L., Markham, B., Richardson, J., Robbins, J., Grant, S.R., and Olson, E.N. (1998). A calcineurin-dependent transcriptional pathway for cardiac hypertrophy. Cell *93*, 215–228.

Muller, C.W., Rey, F.A., Sodeoka, M., Verdine, G.L., and Harrison, S.C. (1995). Structure of the NF-κB p50 homodimer bound to DNA. Nature *373*, 311–317.

Nabel, G., and Baltimore, D. (1987). An inducible transcription factor activates expression of human immunodeficiency virus in T cells. Nature *326*, 711–713.

Navarro, J., Punzon, C., Jimenez, J.L., Fernandez-Cruz, E., Pizarro, A., Fresno, M., and Munoz-Fernandez, M.A. (1998). Inhibition of phosphodiesterase type IV suppresses human immunodeficiency virus type 1 replication and cytokine production in primary T cells: involvement of NF-κB and NFAT. J. Virol. *72*, 4712–4720.

Northrop, J.P., Ho, S.N., Chen, L., Thomas, D.J., Timmerman, L.A., Nolan, G.P., Admon, A., and Crabtree, G.R. (1994). NF-AT components define a family of transcription factors targeted in T-cell activation. Nature *369*, 497–502.

Okamoto, S., Mukaida, N., Yasumoto, K., Rice, N., Ishikawa, Y., Horiguchi, H., Murakami, S., and Matsushima, K. (1994). The interleukin-8 AP-1 and κB-like sites are genetic end targets of FK506-sensitive pathway accompanied by calcium mobilization. J. Biol. Chem. *269*, 8582–8589.

Otwinowski, Z., and Minor, W. (1997). Processing of X-ray diffraction data collected in oscillation mode. Methods Enzymol. *276*, 307–326.

Pereira, L.A., Bentley, K., Peeters, A., Churchill, M.J., and Deacon, N.J. (2000). A compilation of cellular transcription factor interactions with the HIV-1 LTR promoter. Nucleic Acids Res. *28*, 663–668.

Perkins, N.D., Edwards, N.L., Duckett, C.S., Agranoff, A.B., Schmid, R.M., and Nabel, G.J. (1993). A cooperative interaction between NF-κB and Sp1 is required for HIV-1 enhancer activation. EMBO J. *12*, 3551–3558.

Perkins, N.D., Agranoff, A.B., Duckett, C.S., and Nabel, G.J. (1994). Transcription factor AP-2 regulates human immunodeficiency virus type 1 gene expression. J. Virol. *68*, 6820–6823.

Pessler, F., and Cron, R.Q. (2004). Reciprocal regulation of the nuclear factor of activated T cells and HIV-1. Genes Immun. *5*, 158–167.

Piatak, M., Jr., Saag, M.S., Yang, L.C., Clark, S.J., Kappes, J.C., Luk, K.C., Hahn, B.H., Shaw, G.M., and Lifson, J.D. (1993). High levels of HIV-1 in plasma during all stages of infection determined by competitive PCR. Science *259*, 1749–1754.

Ranjbar, S., Tsytsykova, A.V., Lee, S.K., Rajsbaum, R., Falvo, J.V., Lieberman, J., Shankar, P., and Goldfeld, A.E. (2006). NFAT5 regulates HIV-1 in primary monocytes via a highly conserved long terminal repeat site. PLoS Pathog. *2*, e130. Published online December 15, 2006. 10.1371/journal.ppat.0020130.

Robichaud, G.A., Barbeau, B., Fortin, J.F., Rothstein, D.M., and Tremblay, M.J. (2002). Nuclear factor of activated T cells is a driving force for preferential productive HIV-1 infection of CD45RO-expressing $CD4^+$ T cells. J. Biol. Chem. *277*, 23733–23741.

Ross, E.K., Buckler-White, A.J., Rabson, A.B., Englund, G., and Martin, M.A. (1991). Contribution of NF-κB and Sp1 binding motifs to the replicative capacity of human immunodeficiency virus type 1: distinct patterns of viral growth are determined by T-cell types. J. Virol. *65*, 4350–4358.

Shaw, J.P., Utz, P.J., Durand, D.B., Toole, J.J., Emmel, E.A., and Crabtree, G.R. (1988). Identification of a putative regulator of early T cell activation genes. Science *241*, 202–205.

Siekevitz, M., Josephs, S.F., Dukovich, M., Peffer, N., Wong-Staal, F., and Greene, W.C. (1987). Activation of the HIV-1 LTR by T cell mitogens and the trans-activator protein of HTLV-I. Science *238*, 1575–1578.

Simmons, A., Aluvihare, V., and McMichael, A. (2001). Nef triggers a transcriptional program in T cells imitating single-signal T cell activation and inducing HIV virulence mediators. Immunity *14*, 763–777.

Stroud, J.C., and Chen, L. (2003). Structure of NFAT bound to DNA as a monomer. J. Mol. Biol. *334*, 1009–1022.

Stroud, J.C., Lopez-Rodriguez, C., Rao, A., and Chen, L. (2002). Structure of a TonEBP-DNA complex reveals DNA encircled by a transcription factor. Nat. Struct. Biol. *9*, 90–94.

Thali, M., Bukovsky, A., Kondo, E., Rosenwirth, B., Walsh, C.T., Sodroski, J., and Gottlinger, H.G. (1994). Functional association of cyclophilin A with HIV-1 virions. Nature *372*, 363–365.

Verhoef, K., Sanders, R.W., Fontaine, V., Kitajima, S., and Berkhout, B. (1999). Evolution of the human immunodeficiency virus type 1 long terminal repeat promoter by conversion of an NF-κB enhancer element into a GABP binding site. J. Virol. *73*, 1331–1340.

Weissman, D., Barker, T.D., and Fauci, A.S. (1996). The efficiency of acute infection of $CD4^+$ T cells is markedly enhanced in the setting of antigen-specific immune activation. J. Exp. Med. *183*, 687–692.

Wu, Y., Borde, M., Heissmeyer, V., Feuerer, M., Lapan, A.D., Stroud, J.C., Bates, D.L., Guo, L., Han, A., Ziegler, S.F., et al. (2006). FOXP3 controls regulatory T cell function through cooperation with NFAT. Cell *126*, 375–387.

Yamamoto, K.R., Pearce, D., Thomas, J., and Miner, J.N. (1992). Combinatorial regulation at a mammalian composite response element. In Transcriptional Regulation, S.L. McKnight and K.R. Yamamoto, eds. (New York: Cold Spring Harbor Laboratory Press), pp. 1169–1192.

Youn, H.D., Chatila, T.A., and Liu, J.O. (2000). Integration of calcineurin and MEF2 signals by the coactivator p300 during T-cell apoptosis. EMBO J. *19*, 4323–4331.

 ©2008 Elsevier Ltd All rights reserved